

Disassembly sequence planning validated thru augmented reality for a speed reducer

Leonardo Frizziero, Giampiero Donnici, Gian Maria Santi, Christian Leon-Cardenas, Patrich Ferretti, Gaia Pascucci & Alfredo Liverani |

To cite this article: Leonardo Frizziero, Giampiero Donnici, Gian Maria Santi, Christian Leon-Cardenas, Patrich Ferretti, Gaia Pascucci & Alfredo Liverani | (2022) Disassembly sequence planning validated thru augmented reality for a speed reducer, Cogent Engineering, 9:1, 2061321, DOI: [10.1080/23311916.2022.2061321](https://doi.org/10.1080/23311916.2022.2061321)

To link to this article: <https://doi.org/10.1080/23311916.2022.2061321>



© 2022 The Author(s). This open access article is distributed under a Creative Commons Attribution (CC-BY) 4.0 license.



Published online: 28 Apr 2022.



Submit your article to this journal [↗](#)



Article views: 23



View related articles [↗](#)



View Crossmark data [↗](#)



PRODUCTION & MANUFACTURING | RESEARCH ARTICLE

Disassembly sequence planning validated thru augmented reality for a speed reducer

Leonardo Frizziero¹, Giampiero Donnici¹, Gian Maria Santi¹, Christian Leon-Cardenas^{1*}, Patrich Ferretti¹, Gaia Pascucci¹ and Alfredo Liverani¹

Received: 17 November 2021
Accepted: 01 March 2022

*Corresponding author: Christian Leon-Cardenas, Department of Industrial Engineering, ALMA MATER STUDIORUM University of Bologna, I-40136 Bologna, Italy
E-mail: christian.leon2@unibo.it

Reviewing editor: Wenjun Xu, Wuhan University of Technology, Wuhan, Hubei province, China

Additional information is available at the end of the article

Abstract: The lifecycle of a product is getting shorter in today's market realities. Latest developments in the industry are heading towards achieving products that are easy to recycle, by developing further technological advances in raw materials ought to include input from End of Life (EOL) products so a reduction of natural harm could be achieved, hence reducing the overall production environmental footprint. Therefore, the approach taken as a design for environment, a key request nowadays in order to develop products that would ease the reverse manufacturing process leading to a more efficient element recycling for later use as spare parts or remanufacturing. The methodology proposed compares three probable disassembly sequences following a comparison of literature-found procedures between genetic algorithms and as a "state space search" problem, followed by a hybrid approach developed by the authors. Time and evaluation of these procedures reached to the best performing sequence. A subsequent augmented reality disassembly simulation was performed with the top-scored operation sequence with which the user is better able to familiarize himself with the assembly than a traditional paper

ABOUT THE AUTHOR

The Department of Industrial Engineering, at Alma Mater Studiorum University of Bologna promotes the scientific concerns related to the Mechanical Design and Industrial Design Methods by means of state-of-the-art Computer-based Engineering Methodologies like CAD, CAM, CAE, Augmented Reality and related technologies, as well as applications of Advanced Design, QFD, TRIZ, DFSS, DFD, DFA and other industrial product development methods. Other research areas are concerned to Design and Methods of Industrial Engineering englobed by the group including to additive manufacturing optimization and the systematic optimization of product development across the entire organizations.

PUBLIC INTEREST STATEMENT

The study entitled "Disassembly Sequence Planning Validated thru Augmented Reality for a Speed Reducer" was performed to help to better understand the disassembly analyses in a practical way, by performing a digital model-based simulation of the calculated disassembly sequences by means of Augmented Reality (AR) technology. The theory about disassembly planning is very extensive, hence it is challenging to fully realize its feasibility to adopt a given methodology. AR technology in this study is a tool used to better understand the matters of each proposed sequence arrived from a theoretical foundation. This methodology would be keen to aid product designers to practically ease the product development phase to include the product End of Life (EOL) correct handling, so a reduction of natural harm could be achieved, hence reducing the overall production environmental footprint. Therefore, this approach answers towards achieving an efficient circular economy, a key request nowadays to develop products leading to a more efficient element recycling for reuse as spare parts or remanufacturing.

manual, therefore enlightening the feasibility of the top performing sequence in the real world.

Subjects: Industrial Design; Manufacturing & Processing; Mechanical Engineering Design; Mechanical Engineering Design; Operations Management

Keywords: Disassembly; optimization; closed loop; genetic algorithms; metaheuristic method; particle swarm optimizer

1., Introduction

It is widely known that obsolete or discarded products can cause severe environmental pollution if handled improperly. The waste materials of manufacturing companies, which account for 70% of environmental pollution (Lambert, 2003), contain reusable resources that can be recycled and used to generate economic benefits. The recycling and reuse of discarded products has attracted a lot of attention from engineers and scholars around the world. A disassembly planning system is essential for the optimization of these activities, it includes three basic elements: the representation of the product, the search for the sequence and the optimization of the solution.

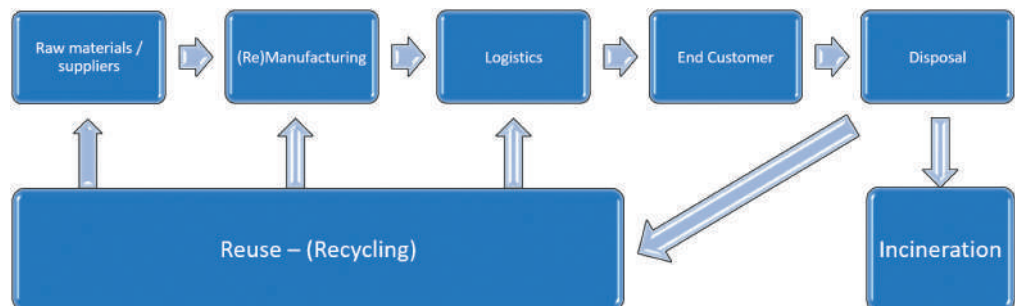
1.1. Design for disassembly

Recently Design for Disassembly has gained a lot of attention due to growing concerns about materials, resources, energy saving and environmental awareness. The widespread diffusion of consumer goods and the shortening of product life cycles have led to the rejection of an unprecedented number of used products. EOL (End Of Life) products contain large quantities of reusable material, which recovery would be beneficial to both the manufacturer and the environment. The reverse production chain is one of the main methods to solve this problem, which mainly involves: remanufacturing of the product, recycling of materials, reuse of components and final disposal, which includes incineration and landfill. Figure 1 shows a closed-loop supply chain (CLSC). It involves the selection of raw and ancillary material suppliers, product partner evaluation, inventory management, market demand, disassembly planning, transport distribution, reverse logistics and then supply chain design. closed cycle. Disassembly is a critical operation in CLSC since recycling, remanufacturing and reuse require the disassembly of EOL products (Meng & Zhang, 2020). The design of the disassembly sequence determines how EOL products are disassembled to recover reusable components and materials, or to separately dispose of parts with harmful substances, such as environmental pollutants.

Further while, it is difficult to obtain an optimal sequence as this process encounters complexity, especially as the number of parts of the assembly increases (such as an automotive product), however a good sequence can be obtained through proper analysis and evaluation. The difficulty of disassembling a product can be attributed to the following factors:

- Accessibility: measure of the ease with which a part can be reached manually or with a tool;

Figure 1. Closed loop supply chain.



- Positioning: the degree of precision required to position the instrument or hand;
- Strength: measure of the effort required to perform the operation;
- Basic time: the time needed to perform the movements of the basic operation without difficulty.

The summary points took into account different combinations of theoretical models and technology in order to arrive to an optimal solution. Starting from the methodology described by (Desai & Mital, 2003) that assigned the weight of time to numerous factors such as the size and shape of the components to be disassembled, weight, frequency of disassembly activities, the need for manpower, postural requirements and handling requirements some materials. A system of scoring has been defined for the elementary operations that are part of the disassembly, taking as reference the simplest operation, that is to remove an easily graspable object without the exertion of a lot of manual force by a trained worker in average condition. Latest state of the art findings of (Chen et al., 2020) considered the optimization of a classic methodology thru a flow balance in the AND/OR network for a large-scale disassembly assessment of a ship diesel engine thru a total operation computing time, by covering multiple nodes and arcs. Other findings using other methodologies like (N. Zhang et al., 2020) that proposed to optimize the sequence thru generating disassembly subsets based on disassembly precedence relationships; as high-quality disassembly sequences can be generated in the solution construction process. Subsequently, (L. Zhang et al., 2021) proposed a selective parallel disassembly sequence planning (SPDSP) methodology, which performs disassembly compared to sequential and Parallel DSP thru a genetic, multi-objective algorithm integrating total disassembly time and costs. Results from (Gunji et al., 2021) included a graph cut-set method to generate sub-assemblies and classify them in order to obtain the most feasible option. Moreover, the fitness equation took into account 6 directional changes.

1.2. Design for environment

Due to the growing concerns on environmental impact, sustainable design methods (Green Design or Design for Environment) have become an important part of the design process. The latter covers the entire life cycle of the product such as design for assembly, supply chain management, life cycle analysis (LCA), design for disassembly, design for remanufacture and planning of the disassembly sequence. All these methods have the same goal, which is to reduce environmental costs and increase economic benefits. The product, in its last phase of life or End Of Life (EOL), as a first step, is generally disassembled to recover the high-value parts: disassembly represents the foundation for most of the treatments of EOL products, therefore it plays a key role in the life cycle of the product. Product disassembly is an expensive process and has a major impact on the final value of EOL products. A product that is difficult to disassemble results in increased costs for reuse or recycling, and the number of parts to be disassembled affects the payback profit. An excellent sequence should be balanced between a “no disassembly” and a “complete disassembly”, as described by (Smith et al., 2016), that underlines an optimal EOL product strategy that minimize disassembly costs would maximize the recycling gains.

Additionally, disassembly represents the “zero phase”: it is essential because it determines the recovery rate in the subsequent treatment processes. Design for Disassembly is an important aspect of the life cycle of a product, it aims to optimize disassembly operations in the product design phase, to reduce maintenance costs or allow for convenient reuse, remanufacturing and recycling. Results gathered from (Hu & Ameta, 2019) stated that optimizing the disassembly process has shown to result in 10–20% of all disassembly-related earnings. Most of the disassembly related gains (80–90%) tend to be determined in the product design phase (Desai & Mital, 2003). Recovery of materials could also lead to environmental issues, as underlined by (Bahubalendruni & Varupala, 2021) that focused on EOL electronics recycling based on a part toxicity matrix, given that part toxicity identification and part recyclability simplifies the number of disassembly levels and results an ideal solution for electronic equipment recycling. Moreover, the authors of (Gunji et al., 2021) applied the type

percentage of disposal based on the origin of the root materials. Other findings of (Anil Kumar et al., 2021) enlightened the emissions minimization through quantification of the toxic gas release into environment is minimized, and quantifying the amount of toxic materials that is separated through systematic disassembly operations, and recycling of the high-value material and quantifying the electricity consumption of the recycling equipment such as shredders.

1.3. Time calculation criteria

In literature the term disassembly depth (Giudice & Fargione, 2007) is also used to indicate the level, the time and costs that become prohibitive with increasing disassembly depth, while revenues tend to stabilize. The profit curve has a maximum point after which it tends to decrease with increasing depth. Therefore, an evaluation of the disassembly sequences plays an important role, also economically, for the reuse of components and their repair. It must be carried out on the basis of a criterion of convenience, and for this work the criterion of times was chosen, with which a more truthful estimate is made of the time it takes to perform each elementary operation during disassembly. In the literature the authors propose different methods for the evaluation of times. This study would consider proposals found in the research of (Mandolini et al., 2018), (Francia et al., 2019), (L. Zhang et al., 2021), (Y. Zhang et al., 2009), and back to the proposal of (Desai & Mital, 2003).

This methodology assigns the weight of time to numerous factors such as the size and shape of the components to be disassembled, as weight, the frequency of disassembly activities, the need for manpower, postural requirements and handling requirements some materials. A system of scoring has been defined for the elementary operations that are part of the disassembly, taking as reference the simplest operation, that is to remove an easily graspable object without the exertion of a lot of manual force by a trained worker in average condition. Subsequent scores were assigned based on the detailed study of the most commonly found disassembly operations.

1.4. The Disassembly Sequence Plan (DSP)

The Disassembly Sequence Plan (DSP) is a sequence of actions that end when the desired disassembly depth is reached. A DSP aims to optimize product recovery by minimizing costs, maximizing recovered material and minimizing disassembly times, using mathematical techniques such as linear programming, dynamic programming and graphics.

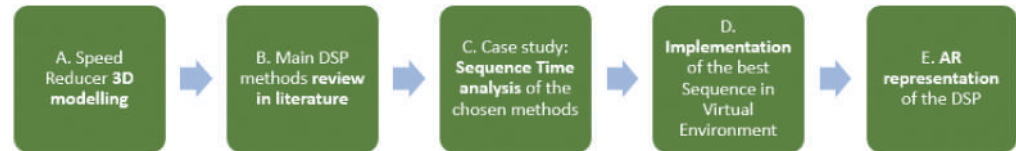
A first rough classification gathered from the methodology proposed by (Lambert, 2003), which developed a procedure based on a combination of previously established methods:

- Modeling methods, which include graphical methods such as, AND/OR graph, first proposed by Homem de Mello in 1980's, as well as Petri nets and matrix-based methods;
- Methods of mathematical programming (MP) and optimization, based on the choice of the optimal option from a set of alternatives;
- Artificial intelligence methods such as Genetic Algorithms (GA), Ant Colony Optimizer (ACO), Scatter Search (SS) and Particle Swarm Optimizer (PSO).

For the generation of the disassembly sequences in the literature several methods are used together, so as to be able to combine the different advantages of both.

This research work develops a first state of the art review on DSP is presented, with an in-depth study of the main methods present in the literature, two models of which will then be applied to the case study of the speed reducer. Then, the mechanical assembly and its modeling on the Creo Parametric software are described, later the sequences described in the first part will be applied to the reducer and a third alternative sequence will be implemented, to then compare the three results obtained through the overall time criterion, after a brief theoretical introduction on the latter. The last part would be the application of augmented reality to the case study. Augmented

Figure 2. Methodology proposed in this study.



Reality (AR) is a technology that allows to see reality in an immersive and realistic environment, it is used by companies to improve the customer or user experience, and as a support vehicle for pre-production planning (Herotech srl. *La Realtà Aumentata nelle aziende*, 2020). AR would become the main tool that helps designers to technically validate the process that has been demonstrated thru the calculated sequences. This also could become the main guide tool for operators in areas like maintenance, and recycling, in order to guide them to better perform their tasks, which would result in higher efficiency in complex component assemblies as engines, and heavy industry machinery. Representation of the methodology is shown in Figure 2.

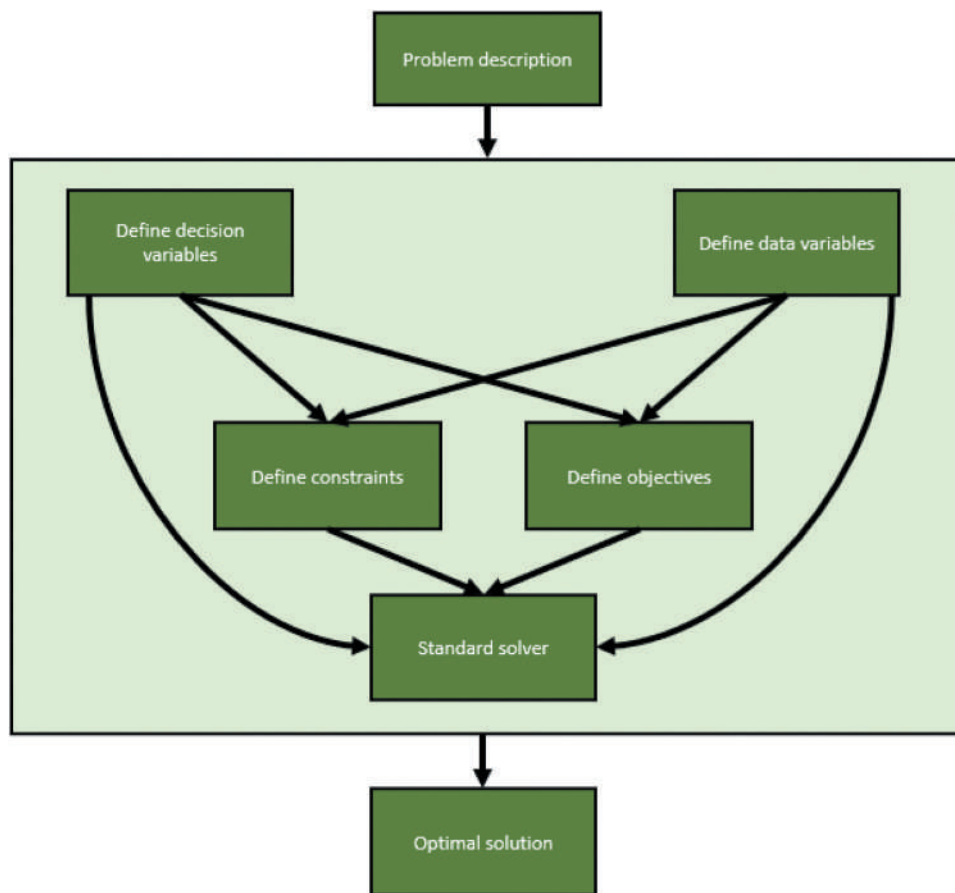
2. Materials and methods

The modeling and representation of a product are essential for obtaining a successful disassembly sequence, as the feasibility of a solution depends on the structure of the product, in which factors are involved such as the relationships between the components (kinematic pairs, joints), the constraints of removal of a component, the geometric structure of a product, a dangerous disassembly feature, tools required for operations, accessibility of space for tools, complexity of components and fasteners to be removed.

Therefore, Mathematical Programming (MP) methods for disassembly sequence design can be linear programming, along with integer linear programming and dynamic linear programming. The flow chart in Figure 3 shows the logic of MP mathematical programming techniques. The characteristic of MP methods is that an optimal solution can be automatically obtained through some commercially available solver, as long as the model is well constructed and reflects reality.

Furthermore, it is worth to mention some of the main modeling methods such as graph-based modeling, AND/OR graph modeling, and matrix-based modeling. The methods were introduced in the study of (Mitrouchev et al., 2015) with graphical representation, the problem of identifying the optimal disassembly and recycling strategy turned into a research problem on the graph; AND/OR graph modeling is important for component disassembly logic. Methodology later adopted by (Mandolini et al., 2018), adapted for Parallel disassembly by (Kim et al., 2018) and subsequently enriched with data mining by (Marconi et al., 2019). The nodes of the graph represent states or goals and their successors are labeled as AND or OR branches. AND successors are secondary goals that must all be met to satisfy the parent goal, while OR branches indicate alternative secondary goals, each of which could satisfy the parent goal. The disadvantage of this method is that as the number of components increases, therefore, it is easy for the graph to become too confusing and ineffective. An oriented arc e_{ij} represents a disassembly operation from node i to node j , while the nodes represent states of the component: the source node is the assembled assembly, the end nodes (or the final node) are the achievement of the disassembly level desired. Lastly, a unique assembly sequence generation (ASG) method was proposed (Bahubalendruni, Gulivindala, Kumar et al., 2019) and further extended for Exploded view generation in CAD software. The ASG follows a deterministic approach to avoid redundant data collection and calculation. The proposed method is effectively applied on products which require such feasible paths of disassembly other than canonical directions. However, because of limitations of the ASG algorithms, a definite method is still unavailable in the computer-aided design (CAD) software, and therefore the

Figure 3. logic of MP mathematical programming techniques



explosion of the product is not found to be in accordance with any feasible disassembly sequence where a disassembly sequence is reverse progression of assembly sequence.

Afterwards, smart optimization methods use algorithms aimed at producing high quality solutions in a reasonable time. They could approximate the exact solution, but they are still valid since they respect times that are not as prohibitive as perhaps the optimal solution might require. An intelligent algorithm uses heuristic strategies, iterative calculations imitating physical or biological phenomena. Citing some intelligent optimization algorithms, we have

Simulated Annealing (SA; Shuyi et al., 2014), (Dowsland & Thompson, 2012), (Hao & Hongfu, 2009), In the algorithm, the reticular defect corresponds to an incorrect combination of two objects. Simulated Annealing aims to find a global minimum when there are multiple local minima and its most common applications are combinatorial problems, in particular scheduling problems.

Genetic Algorithms (GA; Giudice & Fargione, 2007), (Chunming, 2016), (Rickli & Camelio, 2014), (Rickli & Camelio, 2013), (Holland, 1992), they are metaheuristic methods inspired by the principle of natural selection and biological evolution theorized by Charles Darwin, in fact they implement mechanisms conceptually similar to those of the biochemical processes discovered by this science. The fundamental steps of the genetic algorithms start with an initial population of solutions generated randomly and evolving them iteratively.

Ant Colony Optimization (ACO; Dorigo et al., 2006), (Wang et al., 2015), (Luo et al., 2016), (Hu et al., 2017), (X. Zhang et al., 2018), is a probabilistic algorithm aimed to find the optimum sequence to reach a objective. This metaheuristic optimization algorithm served as the start population of some algorithms such as GA and Particle Swarm Optimization (PSO), is random and traditional. ACO may come across local optimization; therefore, it is essential to design operators to get a global, ideal solution.

Particle Swarm Optimization (PSO; Poli et al., 2007), (Zhang & Zhang, 2009), (Xu et al., 2011), (Pornsing & Watanasungsuit, 2014), is an iterative search and optimization heuristic method, whose iterations identify a new “candidate for the best” in the search space, based on a specific quality measure (fitness). It has a very high speed of approaching the optimal solution: its goal is to use the current global information on the extreme, position and individual extreme to guide the particles to the exit. It makes full use of an individual’s experience and swarm to regulate their position.

The proposed methodology undergoes a result comparison of two known methodologies from literature available. To better understand the limitations of the model to analyze, the chosen model was derived after a series of options ruled out by the research team after finding out a great amount of work performed in this area during time. Findings of (Kumar et al., 2021) proposed a novel method to perform geometrical feasibility testing in oblique orientations, an interesting approach for solving problems of disassembly sequence whereas actual part location is not coincident with any of the 6 axis. and later research by (Gulivindala, Bahubalendruni, Inkulu et al., 2021) suggested the Extended Part Concatenation Method to solve both sub-assembly detection to perform a linear assembly sequence planning. but the proposed method could not be adapted to the physical constraints of the speed reducer. The increasing quantity of calculation needed for obtaining the best result in complex assemblies was discussed with the research of (Bahubalendruni, Gulivindala, Varupala et al., 2019) also that outlined the existing sub-assembly detection methods and performed a linear assembly sequence planning. However, the proposed method performed an assembly sequence plan by integrating sub-assembly detection. This research team also conducted an application of Artificial Intelligence (Bahubalendruni & Biswal, 2018) in order to better obtain all valid assembly sequences and reached an optimized assembly sequence for a given assembled product. Four basic predicates namely “liaison predicate, geometrical feasibility, mechanical feasibility, and stability” were considered to validate each sequence.

Criteria taken for the methodology development

- Assumptions taken before generating a disassembly sequence help to constrain the complexity, so the flexibility from each method could be exploited. The hypothesis followed in both methods are listed below.
- The method should be established by state of the art, proven representation models, that follow defined steps, enabling reproducibility and comparability
- No change in the relative position of the subassembled parts at all phases.
- Non-destructive disassembly or “reverse assembly” approach.
- Part movements during assembly operations are ideal assuming no gravitational and friction forces are considered.
- The method should provide specific information about the fasteners used to connect each component and highlight when fastener reusability/reversibility is not ensured
- Matrices with no interference would be generated considering straight line part movements along six main directions on three axes.
- The physical connectors are considered as secondary parts (screws) connecting pins, which are numbered and placed next to complete set of primary parts.
- Take into account rotation of parts and change of tooling

Moreover, the first sequence approaches the sequential, manual work Disassembly Sequence Planning (DSP) problem with a PSO, method that literature findings shown to be first presented by Eberhart and Kennedy in 1995, followed by other research including (Zhong et al., 2011), and further developed in the research of (Kheder, Trigui, Aifaoui et al., 2018), (Kheder, Trigui, Aifaoui et al., 2017) and (Guo et al., 2019); this metaheuristic method would engage following characteristics:

- Partial, Sequential Dissassembly
- Graph-based method with a Dissassembly tree,
- Building method: 6-direction Matrix-based Method, Disassembly interference matrix
- Manual Pre-processing times
- Accounting time required for changing tools, tooling penalty
- State the revenue increase of a salvaged component undamaged by disassembly
- PSO Velocity and position of each particle are updated in the iteration
- Optimization method: Dijkstra's algorithm (DA)—A typical algorithm to solve the shortest path problem
- Construction of a component-fastener graph (Figure 4) to describe overall classification of components into two categories, functional components and fasteners;
- Development of the interference matrix (Table S2) to determine the removable components and implementation of a disassembly sequence of functional components based on the Dijkstra algorithm;
- Presentation of the disassembly sequence, which also includes fasteners, based on Particle Swarm Optimization (PSO).

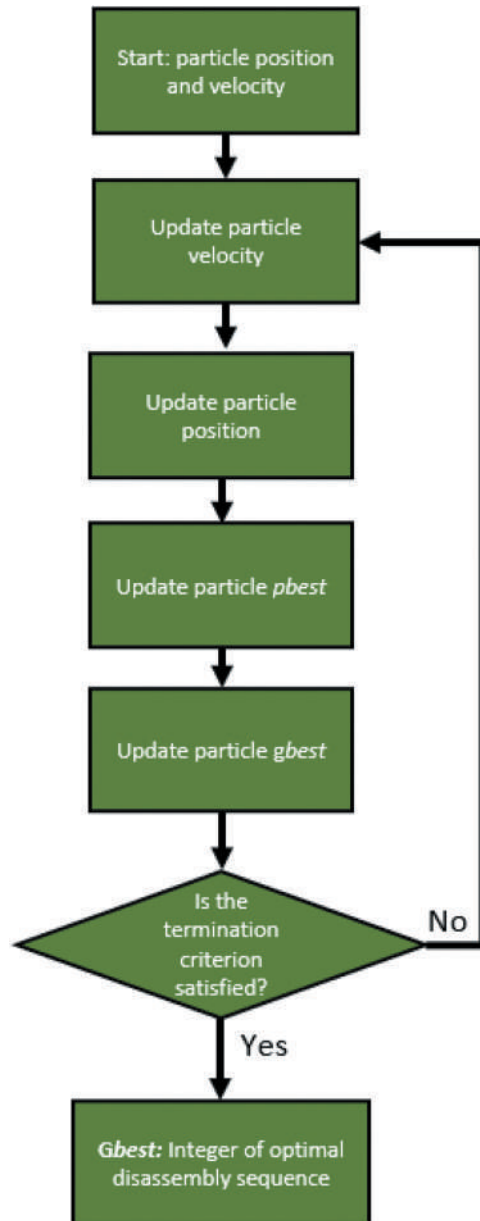
The component-fastener graph is an undirected graph used to describe large overall structures, classifying all components into two categories: fastening components and functional elements. The vertices of the graph represent the functional components, while the arcs represent the fasteners: an arc connects two nodes as a fastener connects two components. The chart may also contain information on disassembly tools and related expenses, which are very helpful in planning the disassembly sequence as changing disassembly tools for different fasteners will increase time and cost. Disassembly costs, which represent the difficulty of removing a component, are directly proportional to the disassembly times and costs, which can be minimized, for example, by limiting the number of tool changes as much as possible.

Moreover, the disassembly sequence was obtained as a “state space search” problem. State space search is a process in which successive configurations or states of an instance are considered, with the intention of finding an objective configuration (or state) with a certain property defined previously (Poole & Mackworth, 2010). This procedure is described in the flow diagram of Figure 5.

Subsequently, a component's removal path can be obstructed by other components in the area. If there were at least one one-direction path of the six directions of geometric space, which are +X, -X, +Y, -Y, +Z and -Z, which is not hindered by other components, we would consider the component to be removable.

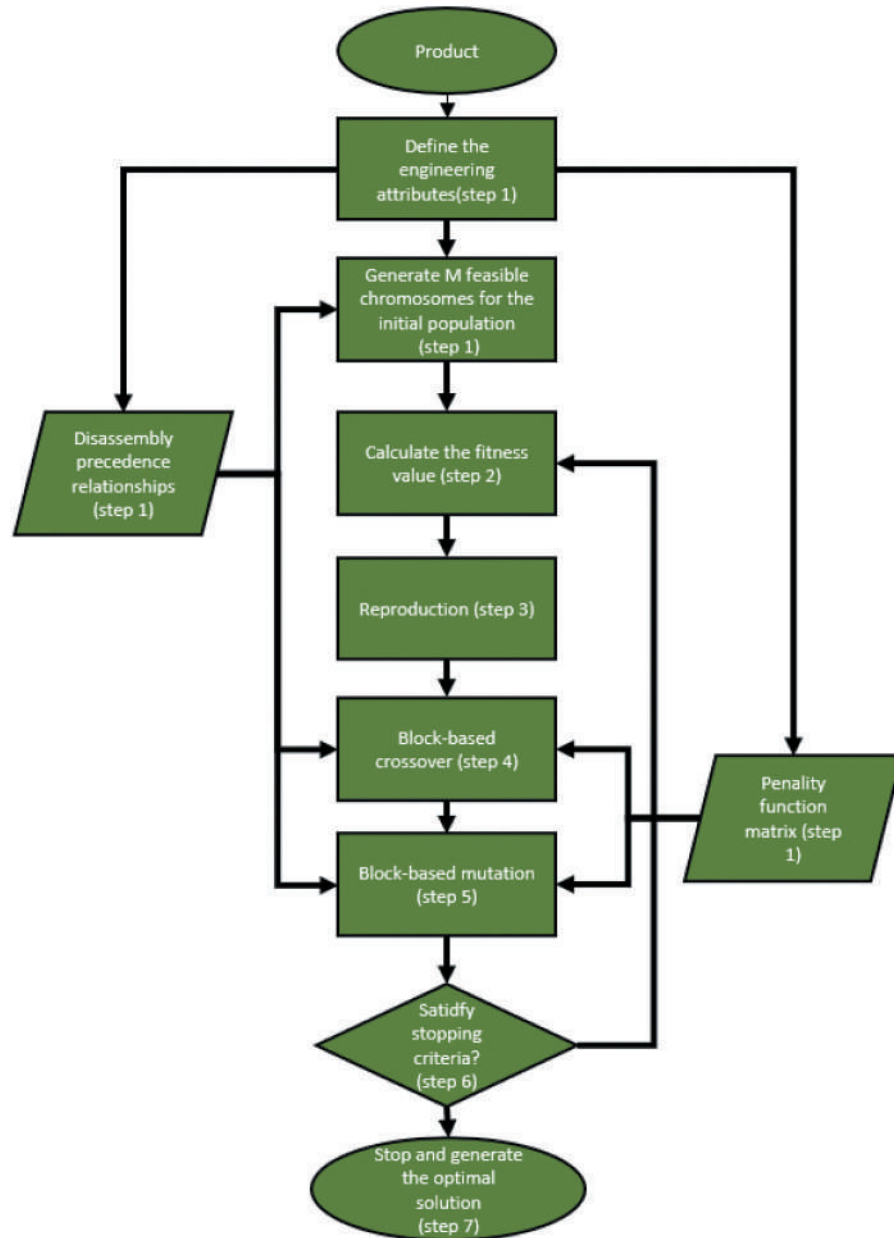
The mathematical calculus of this model uses the interference matrix, used to determine the removal capability of every component. This is represented by: $D = (d_{ij})_{n \times 6}$ where d_{ij} ($i = 1, 2, \dots, n; j = 1, 2, \dots, 6$) is the total number of functional components that obstruct the removal path in the j-th direction of the i-th functional component. A status space search problem is created that, would be solved by means of the classic method of Dijkstra's algorithm and the initial disassembly state can be assumed as {0}. For example, if the status is {1,4,5} it means that

Figure 4. Speed reducer assembly rendering.



components 1, 4 and 5 have already been removed. For each functional component, the sum of the disassembly costs of all the components in that precise state of disassembly must be indicated, so as to be able to help in the choice. When the target component (in the case of selective disassembly) or the last component (for total disassembly) appear in the disassembly state, the procedure ends. The optimal disassembly sequence, i.e. the final disassembly state, ensures that the sum of the disassembly costs of all components reaches the minimum value, which value is indicated by the evaluation function $f(\cdot)$. The evaluation function is defined in each node as the sum of the disassembly costs of all the components that are part of such disassembly state, therefore for each step of the status space searching the functional component that guarantees the lowest $f(\cdot)$ is chosen. A disassembly sequence of n components can be expressed by a complete permutation of n numbers, which corresponds to an integer between 0 and $n! - 1$ ($n!$ Indicates the factorial of n) thanks to the generation of the lexicographic permutation.

Figure 5. First sequence model flux diagram.



Moreover, the position of each particle and the velocity are defined to determine the initial population, the position of the j -th particle is given by the equation: $POS_j = round(rand \times (n! - 1))$.

where $rand$ indicates a random number from a uniform distribution (Lambert, 2003), while $round$ is a function that rounds to the nearest integer.

The speed of the j -th particle is given by the equation: $VEL_j = -(n! - 1) + 2(n! - 1) \times rand$

Where two optimal values “ $pbest_j$ ” and “ $gbest$ ” are chosen to update the values of each particle. “ $pbest_j$ ” is the optimal position of the j -th particle from the last iteration, while “ $gbest$ ” is the

optimal position of the swarm from the last iteration. The velocity of the j-th particle at the k-th iteration is given by:

$$VEL_j^{(k)} = \omega^{(k)} \times VEL_j^{(k-1)} + 2 \times rand \times (pbest_j^{(k-1)} - POS_j^{(k-1)}) + 2 \times rand \times (gbest^{(k-1)} - POS_j^{(k-1)})$$

where ω is the weight of the speed of the last iteration. To obtain the optimal value quickly ω should tend to 1 at the beginning and reaching 0 at the end of the iterations.

Afterwards, the position of the j-th particle in the k-th iteration is given by the equation:

$$POS_j^{(k)} = round(VEL_j^{(k)} + POS_j^{(k-1)})$$

The updates of “pbestj” and “gbest” must be consistent with the fitness function $f(\cdot)$, because if

$f(POS_j^{(k)}) < f(pbest_j^{(k-1)})$, then $POS_j^{(k)}$ becomes $pbest_j^{(k)}$, otherwise $pbest_j^{(k-1)}$ becomes $pbest_j^{(k)}$. When the iteration stops, the “gbest” is the optimal position of the particle, i.e. the integer corresponding to the optimal disassembly sequence, and in this situation, the difference between the fitness function of “gbest” in the final iteration and the previous iteration is a very small number. The termination condition is in fact given by:

$$|f(gbest^{(l)}) - f(gbest^{(l-1)})| < \epsilon$$

Afterwards, the second sequence is taken from the research of Tseng et al. (Tseng et al., 2018), which proposes a block-based GA for the planning of disassembly sequences, based on the comparison between the Kongar and Gupta genetic algorithm and the Dijkstra algorithm. Similar to the approach given by Gulivindala, Anil Kumar, et al. (Gulivindala, Bahubalendruni, Chandrasekar et al., 2021) that included a genetic algorithm feasibility by integrating with the proposed priori crossover operator. An optimality function is defined to reduce disassembly effort by considering directional changes as parameters.

The authors of this article highlighted a point of inefficiency of traditional GA, namely that random search addresses the problem of a wide range of possible solutions. To improve the quality of the solution, they therefore propose an algorithm based on the concept of block (block-based), which helps to skip the local solution and processes the search activity on the basis of an objective function and a penalty function. The fitness function guides you in the search for a better direction, so as to make it easier to find the optimal solution and improve the algorithm in terms of efficiency. The procedure for the GA based on blocks is divided into seven key steps, as detailed on Figure 6 schematizes the logic for the genetic algorithm based on blocks.

Moreover, the crossover and mutation mechanisms are characteristic of GA, which are applied in this discussion using block-based rules. The crossover is mainly structured in the following phases:

1. The size of the blocks is chosen, which are simply “portions of sequences”, which then divide the sequence into n-blocksize + 1 blocks (with n number of elements in the sequence);
2. Two parent sequences were selected, which are divided into n-blocksize + 1 blocks, and then the fitness function of each block is calculated. The block with the best function value will become the optimal block;

3. The optimal block of Parent 1 is fixed for the Offspring 1 offspring, the optimal block of Parent 2 is fixed for the Offspring 2 offspring. To complete the chromosome, Parent 1 is reproduced for the Offspring 2 offspring and Parent 2 for the Offspring 2 offspring. Offspring 1 offspring;
4. Search for repetitive and missing codes in child chromosomes;
5. Eliminate repetitive codes;
6. Calculate the fitness function of the possible positions for the insertion of the missing genetic codes;
7. Select the best position for inserting the missing genetic codes;
8. Individually insert the missing genetic codes in the generation of the child chromosomes.

Figure 7 shows a simple example of a crossover for a sequence of elements.

Lastly, the block-based mutation mechanism adopted a multiple point method. The key steps were as follows:

1. Randomly select a chromosome point for the mutation point and provisionally remove it from the chromosome;
2. Find the range for the insertion of the mutation point, so that feasible solutions would be generated;
3. Calculate the increase in the value of the fitness function for all the mutation points in the identified range;
4. Find the best value of the fitness function for the insertion of the mutation point
5. Repeat the previous steps for m times, in which m is defined beforehand.

2.1. Case study: speed reducer

The disassembly sequences would be calculated for a speed reducer, which is a mechanical system that transmits power to the shaft, modulating it as needed and adjusting the output rotation speed according to the characteristics of the gears. They are usually formed by a gearbox casing; ie a container in which a series of gears are housed responsible for reducing the rotation speed of the input shaft (transmission shaft; RS Components S.r.l, 2020). In this project, a parallel axis speed reducer is studied, in which there are three shafts that house a total of four cylindrical helical

Figure 6. Model for the GA based on blocks (Second sequence).

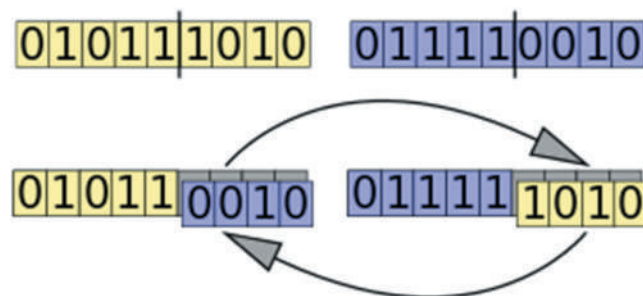
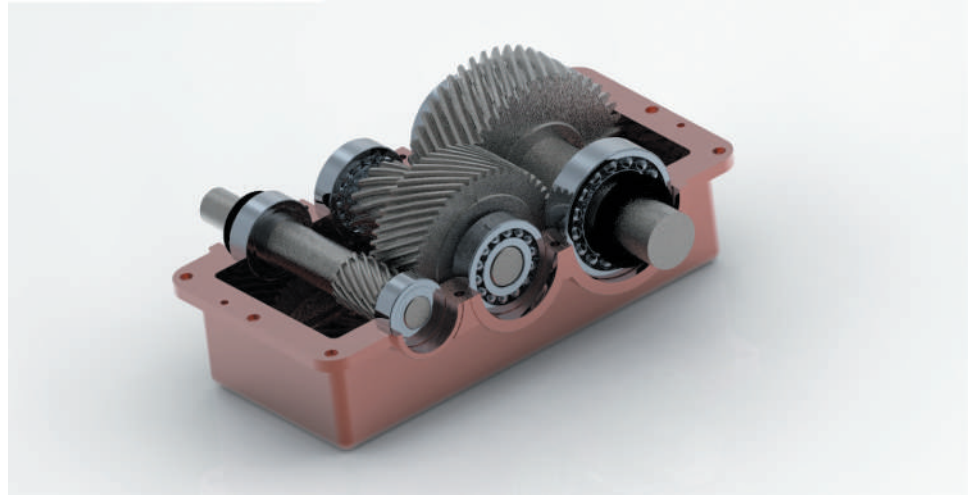


Figure 7. crossover example for an element sequence.



gears, similar to that shown by Barone et al. (Barone et al., 2020). Table 1 shows the bill of materials (BOM).

The casing is made up of two pieces held together by a series of screws. The twelve screws are of three different types, distinguished by the diameter. In the mechanical drawing, the diameter of a screw is designated by the letter “M” followed by the measurement expressed in millimeters which corresponds to the external diameter of the screw body (i.e. the one including the thread). The three shafts at the ends are wedged inside six bearings, which are mechanisms thanks to which the friction between two rotating objects is reduced, in the case of the study of the shafts hosting the gear wheels, as explained by Callegari et al. (Callegari et al., 2013). They consist of two rings of different diameters, one external and one internal, within which are positioned a series of rolling elements, balls or rollers, which roll in special tracks obtained in the rings, and a spacer cage which has the purpose of maintaining the rolling elements at a suitable distance from each other.

Afterwards, the design of each part of the Speed Reducer on Table 1 was designed and assembled with PTC Creo Parametric—student limited license. Creo Parametric has the ability to render models and provide a more realistic image of the objects created. For the assembly, an “.asm” extension file was created and defined the relative position of the components, importing them one at a time, imposing constraints (such as tangent, coincident, normal, etc.) on the surfaces. Figure 4 shows the rendering of the entire assembly except screws, upper casing and covers.

2.1.1. First Disassembly Sequence

The component-fastener graph of the speed reducer is represented in Figure 8. The reducer has only screws as fastening elements, as all other components are connected with interlocking mechanisms. Subsets have been identified, indicated with the letter “S” followed by a number for identification. Next to the graph is the table with information on the identification code of the components or the set of components to facilitate understanding of the graph.

$$D = (d_{ij})_{n \times 6} \quad (1)$$

Table 1. Speed reducer bill of materials

Cod.	Description	Quantity
1	Shaft 1	1
2	Shaft 2	1
3	Shaft 3	1
4	End cover 1	1
5	End cover 2	1
6	End cover 3	2
7	End cover 4	1
8	End cover 5	1
9	Spacer 1	1
10	Spacer 2	1
11	Spacer 3	1
12	Bottom carcass	1
13	Upper carcass	1
14	Sealing ring 1	1
15	Sealing ring 2	1
16	Bearing 2206E	1
17	Bearing 2205E	1
18	Bearing 1306E	2
19	Bearing 2209E	1
20	Bearing 1309E	1
21	Screw M6x20	2
22	Screw M8x50	4
23	Screw M10x20	6

The interference matrix (Table 2) is represented by the equation 1 in which each cell indicates the number of functional components that obstruct the removal of the *i*-th component in the *j*-th direction. If a zero appears, it means that component can be removed immediately in that direction. The ordering rule corresponds to that used in dictionaries, even if it is extended to any set of symbols (Van Zanten, 1997). It could be described as a state space search problem, so at each change of state, which in this case corresponds to the removal of a component, the interference matrix must be updated, to have a clear picture of which components can be removed in the next step. Table 2 shows the initial interference matrix, therefore a completely constructed assembly, in which the cells left empty indicate that that component can never be removed in that direction, or that it would not make sense to do so. A subsequent fastener incidence matrix was performed in Table 3 to evaluate the constraints criteria of fasteners adopted in this the model.

Furthermore, Dijkstra’s algorithm was used to solve the status space search problem. It was necessary to define an evaluation function for the choice of components to be removed. A method for evaluating disassembly costs was followed after the study of Tseng et al. (Tseng et al., 2018). The square-shape penalty matrix was defined, seen in Table 4, in which each cell reports the disassembly costs in case the *i*-th component is removed after the *k*-th component, with *i* ≠ *k*. The costs are related to the change of direction of disassembly and to the tool change. It is filled in only under the main diagonal because it is symmetrical. Furthermore, the penalty function matrix, was obtained by adding the values obtained from the following two criteria

- For a 90 ° change of disassembly direction a score of 1 is assigned, for a 180 ° change a score of 2 is assigned.

Figure 8. Speed reducer component-fastener graph and item description.

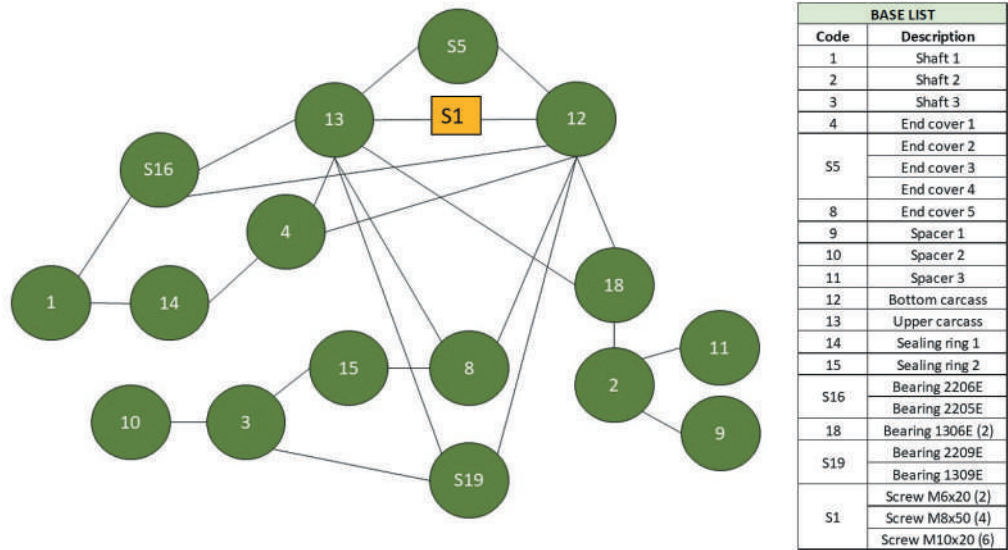


Table 2. Initial Interference Matrix

INITIAL INTERFERENCE MATRIX

Cod.	Component	.+X	.-X	.+Y	.-Y	.+Z	.-Z
1	Shaft 1			16			
2	Shaft 2			15			
3	Shaft 3			16			
4	End cover 1						0
5	End cover 2					0	
6a	End cover 3 a						0
6b	End cover 3 b					0	
7	End cover 4						0
8	End cover 5					0	
9	Spacer 1						2
10	Spacer 2						2
11	Spacer 3					2	
12	Bottom carcass			33			
13	Upper carcass			12			
14	Sealing ring 1						1
15	Sealing ring 2					1	
16	Bearing 2206E			14		3	2
17	Bearing 2205E			14		1	4
18a	Bearing 1306E a			14		3	1
18b	Bearing 1306E b			14		1	3
19	Bearing 2209E			14		4	1
20	Bearing 1309E			14		2	3
21	Screw M6			0			
22	Screw M8			0			
23	Screw M10			0			

Table 3. Fasteners Incidence Matrix
INCIDENCE MATRIX

			Fasteners						
			End cover 1	End cover 2	End cover 3 a	End cover 3 b	End cover 4	End cover 5	Screws
			C4	C5	C6A	C6B	C7	C8	S1
Functional Components	Shaft 1	C1	1	0	0	0	0	0	0
	Shaft 2	C2	0	0	0	0	0	0	0
	Shaft 3	C3	0	0	0	0	0	1	0
	Spacer 1	C9	0	0	0	0	0	0	0
	Spacer 2	C10	0	0	0	0	0	0	0
	Spacer 3	C11	0	0	0	0	0	0	0
	Bottom carcass		1	1	1	1	1	1	1
	Upper carcass	C13	1	1	1	1	1	1	1
	Sealing ring 1	C14	1	0	0	0	0	0	0
	Sealing ring 2	C15	0	0	0	0	0	1	0
	Bearing 2206E	C16	0	0	0	0	0	0	0
	Bearing 2205E	C17	0	0	0	0	0	0	0
	Bearing 1306E a	C18A	0	0	0	0	0	0	0
	Bearing 1306E b	C18B	0	0	0	0	0	0	0
	Bearing 2209E	C19	0	0	0	0	0	0	0
Bearing 1309E	C20	0	0	0	0	0	0	0	

- For the disassembly method, a score of 1 is assigned for the tool change.

However, the disassembly sequence is shown in Table 5, each part added a C letter and related to that step, and the disassembly expense is counted according to the group of elements in which is related to. The total evaluation function was gathered by adding these values which in this case was equal to 7.

2.1.2. Second disassembly sequence

Second Sequence:

The second disassembly sequence was gathered by following the GA based on the concept of blocking performed by Tseng et al. (Tseng et al., 2018), it proved to be a reasonably quick method to implement manually, as it helped to skip the local solution and the search was carried out according to a penalty function, that was the same one used for the previous sequence. However, it was essential to identify the disassembly directions, inserted within a matrix represented in Table 6 for the construction of the penalty function. The model of this sequence is displayed before on Figure Figure 4.

Table 4. Penalty Matrix

PENALTY MATRIX

	1	2	3	4	5	6a	6b	7	8	9	10	11	12	13	14	15	16	17	18a	18b	19	20	21	22	23
Shaft 1	1	0																							
Shaft 2	2	0	0																						
Shaft 3	3	0	0	0																					
End cover 1	4	1	1	1	0																				
End cover 2	5	1	1	1	2	0																			
End cover 3 a	6a	1	1	1	0	2	0																		
End cover 3 b	6b	1	1	1	2	0	2	0																	
End cover 4	7	1	1	1	0	2	0	2	0																
End cover 5	8	1	1	1	2	0	2	0	2	0															
Spacer 1	9	1	1	1	0	2	0	2	0	2	0														
Spacer 2	10	1	1	1	0	2	0	2	0	2	0	0													
Spacer 3	11	1	1	1	2	0	2	0	2	0	2	2	0												
Bottom carcass	12												0												
Upper carcass	13	0	0	0	1	1	1	1	1	1	1	1	0												
Sealing ring 1	14	1	1	1	0	2	0	2	0	2	0	2	1	0											
Sealing ring 2	15	1	1	1	2	0	2	0	2	0	2	2	1	2	0										
Bearing 2206E	16	1	1	1	0	2	0	2	0	2	0	2	1	0	2	0									
Bearing 2205E	17	1	1	1	2	0	2	0	2	0	2	2	1	2	0	2	0								
Bearing 1306E a	18a	1	1	1	0	2	0	2	0	2	0	2	1	0	2	0	2	0							
Bearing 1306E b	18b	1	1	1	2	0	2	0	2	0	2	2	1	2	0	2	0	2	0						
Bearing 2209E	19	1	1	1	0	2	0	2	0	2	0	2	1	0	2	0	2	0	2	0	2	0			
Bearing 1309E	20	1	1	1	2	0	2	0	2	0	2	2	1	2	0	2	0	2	0	2	0	2	0		
Screw M6	21	1	1	1	2	2	2	2	2	2	2	2	1	2	2	2	2	2	2	2	2	2	2	0	
Screw M8	22	1	1	1	2	2	2	2	2	2	2	2	1	2	2	2	2	2	2	2	2	2	2	1	0
Screw M10	23	1	1	1	2	2	2	2	2	2	2	2	1	2	2	2	2	2	2	2	2	2	2	1	0

Table 5. First Disassembly Frequency

Components that minimize $f(\cdot)$	Chosen Sequence	Evaluation function $f(\cdot)$	C20	C20	0
C21	C23		C4	C4	2
C22			C6a		
C23			C7		
C21	C22	1	C14	C7	0
C22			C6a		
C21	C21	1	C7		
C13	C13	1	C14	C19	0
C4	C5	1	C6a		
C5			C19		
C6a			C14	C10	0
C6b			C6a		
C7			C10		
C8			C14	C14	0
C8	C8	0	C6a		
C17			C6a	C6a	0
C6b			C16		
C17	C6b	0	C16	C18a	0
C6b			C18a		
C15			C16	C16	0
C17	C17	0	C9		
C15			C9	C9	0
C18b			C1	C2	1
C15	C18b	0	C2		
C18b			C3		
C15	C15	0	C1	C3	0
C11			C3		
C11	C11	0	C1	C1	0
C20			TOTAL $f(\cdot)$		7

Table 6. Part disassembly orientation

DISASSEMBLY DIRECTION		
Cod.	Description	Direction
1	Shaft 1	.+y
2	Shaft 2	.+y
3	Shaft 3	.+y
4	End cover 1	.-z
5	End cover 2	.+z
6A	End cover 3a	.-z
6B	End cover 3b	.+z
7	End cover 4	.-z
8	End cover 5	.+z
9	Spacer 1	.-z
10	Spacer 2	.-z
11	Spacer 3	.+z
12	Bottom carcass	
13	Upper carcass	.+y
14	Sealing ring 1	.-z
15	Sealing ring 2	.+z
16	Bearing 2206E	.-z
17	Bearing 2205E	.+z
18A	Bearing 1306E a	.-z
18B	Bearing 1306E b	.+z
19	Bearing 2209E	.-z
20	Bearing 1309E	.+z
S1	Screw M6x20	.+y
	Screw M8x50	.+y
	Screw M10x20	.+y

The oriented graph that makes the precedence relations explicit (Figure Figure 9) for which all the screws were grouped in a subset called “S1” and to facilitate reading I have inserted the letter “C” before the component code. The creation of this graph was a fundamental step for the implementation of the algorithm since in the development of the sequence chose only the components admissible to be removed and avoided post controls. The next step involves the generation of M chromosomes eligible as initial parents. Taking M = 3 therefore 3 feasible disassembly sequences were used to calculate the fitness function, the blocks with the lowest fitness function (F.F.) are the optimal blocks that are not separated during the crossover operation. Following the steps that describe the crossover mechanism described in the second sequence, 3 “Offspring” sequences were created as shown in Figure Figure 10. Also the fitness function could decrease by about five points on average with the crossover mechanism alone.

Thereafter, after arriving a total of six sequences, from whom only two were selected sequences to continue the algorithm, choosing those that minimized the function, namely “Sequence 1” and “Offspring 3”. With the latter I performed the operations described by the mutation mechanism, managing to generate a sequence with the lowest value fitness function ever found. These steps are shown in Figure Figure 11. For Sequence 1 it was not possible to change the position of any element, and the value of the fitness function remained 17. With the sequence Offspring 3 It was able to modify the position of two components, decreasing the value of the fitness function by 4, arriving at 11. The red cells indicated the component that has just moved out of position. In carrying out these

Table 7. Time evaluation chart for chosen sequence time

TASK No.	PART No.	TASK	TOOL	DISASSEMBLY FORCE				MATERIAL HANDLING			REQUIREMENT OF TOOLS		ACCESSIBILITY OF JOINTS		POSTITIV ONING	TOTAL TASK	NOTE		
				Push/pull operations with hand	Twisting and push/pull op. with hand	Inter-surface friction	Inter-surface wedging	Material stiffness	Component size	Component weight	Component symmetry	Force exertion	Torque exertion	Dimensions				Locations	
1a	21	Un	Fw	0	2	0	0	0	0	2	2	0.8	0	2	1	1	1.2	12	Remove screw M6
1b	21	Un	Fw	0	2	0	0	0	0	2	2	0.8	0	2	1	1	1.2	12	Remove screw M6
1c	22	Un	Fw	0	2	0	0	0	0	2	2	0.8	0	2	1	1	1.2	12	Remove screw M8
1d	22	Un	Fw	0	2	0	0	0	0	2	2	0.8	0	2	1	1	1.2	12	Remove screw M8
1e	22	Un	Fw	0	2	0	0	0	0	2	2	0.8	0	2	1	1	1.2	12	Remove screw M8
1f	22	Un	Fw	0	2	0	0	0	0	2	2	0.8	0	2	1	1	1.2	12	Remove screw M8
1g	23	Un	Fw	0	2	0	0	0	0	2	2	0.8	0	2	1	1	1.2	12	Remove screw M10
1h	23	Un	Fw	0	2	0	0	0	0	2	2	0.8	0	2	1	1	1.2	12	Remove screw M10
1i	23	Un	Fw	0	2	0	0	0	0	2	2	0.8	0	2	1	1	1.2	12	Remove screw M10
1j	23	Un	Fw	0	2	0	0	0	0	2	2	0.8	0	2	1	1	1.2	12	Remove screw M10
1k	23	Un	Fw	0	2	0	0	0	0	2	2	0.8	0	2	1	1	1.2	12	Remove screw M10

(Continued)

Table 7. (Continued)

DISASSEMBLY EVALUATION CHART

TASK No.	PART No.	TASK	TOOL	DISASSEMBLY FORCE					MATERIAL HANDLING			REQUIREMENT OF TOOLS		ACCESSIBILITY OF JOINTS		POSTITIVONING	TOTAL TASK	NOTE	
				Push/pull operations with hand	Twisting and push/pull op. with hand	Inter-surface friction	Inter-surface wedging	Material stiffness	Component size	Component weight	Component symmetry	Force exertion	Torque exertion	Dimensions	Locations				
1l	23	Un	Fw	0	2	0	0	0	0	2	2	0.8	0	2	1	1	1.2	12	Remove screw M10
2a	13	Pu	/	3	0	0	0	0	0	4	3	4	2	2	2	1.6	0.2	19.8	Remove Top Cover
3f	4	Pu	/	2	0	1	0	0	0	2	2	0.8	2	0	1	2	2	14.8	Remove the cover
3a	6a	Pu	/	2	0	1	0	0	0	2	2	0.8	2	0	1	1.2	1.8	13.8	Remove the cover
3b	7	Pu	/	2	0	1	0	0	0	2	2	0.8	2	0	1	1.2	1.8	13.8	Remove the cover
3d	8	Pu	/	2	0	1	0	0	0	2	2	0.8	2	0	1	2	1.8	14.6	Remove the cover
3c	6b	Pu	/	2	0	1	0	0	0	2	2	0.8	2	0	1	1.2	1.8	13.8	Remove the cover
3e	5	Pu	/	2	0	1	0	0	0	2	2	0.8	2	0	1	1.2	1.8	13.8	Remove the cover
7a	15	Pu	Lp	0	0	0	0	4.5	2	2	0.8	3	0	3	1.6	1.3	5.5	20.7	Remove sealing ring
7b	14	Pu	Lp	0	0	0	0	4.5	2	2	0.8	3	0	3	1.6	1.3	5	20.2	Remove sealing ring
4d	16	Pu	Pr	0	0	5	0	0	2	2	0.8	3	0	3	2.2	1	5	21	Remove bearing 2206E

(Continued)

Table 7. (Continued)

DISASSEMBLY EVALUATION CHART

TASK No.	PART No.	TASK	TOOL	DISASSEMBLY FORCE					MATERIAL HANDLING			REQUIREMENT OF TOOLS		ACCESSIBILITY OF JOINTS		POSITIONING	TOTAL TASK	NOTE	
				Push/pull operations with hand	Twisting and push/pull op. with hand	Inter-surface friction	Inter-surface wedging	Material stiffness	Component size	Component weight	Component symmetry	Force exertion	Torque exertion	Dimensions	Locations				
4a	18a	Pu	Pr	0	0	5	0	0	0	2	2	0.8	3	0	2.2	1.2	4.5	20.7	Remove bearing 1306E
4e	19	Pu	Pr	0	0	5	0	0	0	2	2	0.8	3	0	2.2	1.2	4.5	20.7	Remove bearing 2209E
4c	20	Pu	Pr	0	0	5	0	0	0	2	2	0.8	3	0	2.2	2	4.5	21.5	Remove bearing 1309E
4b	18b	Pu	Pr	0	0	5	0	0	0	2	2	0.8	3	0	2.2	1.2	4.5	20.7	Remove bearing 1306E
4 f	17	Pu	Pr	0	0	5	0	0	0	2	2	0.8	3	0	2.2	1.2	4.5	20.7	Remove bearing 2205E
5b	11	Pu	/	0.5	0	0	0	0	0	1.6	1	0.8	1	0	1.6	1.2	1.5	9.2	Remove spacer
5c	10	Pu	/	0.5	0	0	0	0	0	1.6	1	0.8	1	0	1.6	2	1.2	9	Remove spacer
5a	9	Pu	/	0.5	0	0	0	0	0	2	1	0.8	1	0	1.6	1.2	1.2	9.3	Remove spacer
6c	1	Pu	/	1	0	0	0	0	0	3.5	2.5	0.5	1	0	1.3	2	1	12.8	Remove shaft
6a	2	Pu	/	1	0	0	0	0	0	3.5	2.5	0.5	1	0	1.3	1	1	11.8	Remove shaft
6b	3	Pu	/	1	0	0	0	0	0	3.5	2.5	0.5	1	0	1.3	1	1	11.8	Remove shaft
													Total time (TMU)		478.5				
													Unit value (TMU)		0.036				
													Estimated time (ET) (sec.)		172.26				
													ET in minutes		2.871				

Figure 9. Oriented graph for priority assessment.

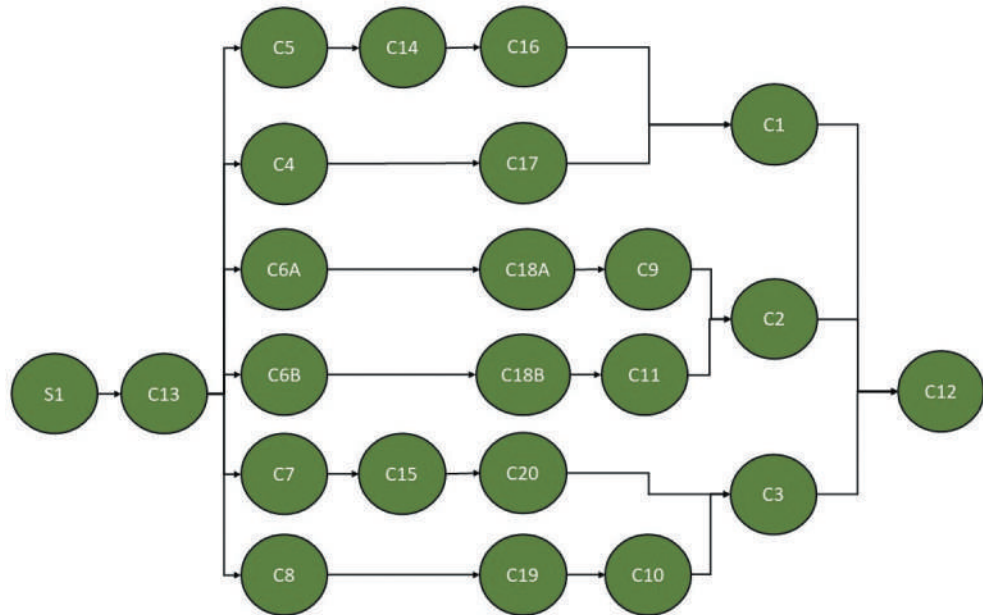


Figure 10. “Offspring” Sequences

OFFSPRING 1	S1	C13	C5	C4	C14	C16	C17	C1	C6A	C18A	C9	C6B	C18B	C7	C15	C20	C19	C8	C11	C10	C2	C3	C12	TOTAL		
F.F.	1	1	2	0	0	2	1	1	0	0	2	0	2	2	0	2	2	0	2	2	0	2	1	0	0	21
OFFSPRING 2	S1	C13	C5	C4	C14	C16	C17	C1	C6A	C6B	C18A	C7	C8	C18B	C20	C19	C9	C11	C10	C1	C2	C3	C12	TOTAL		
F.F.	1	1	2	0	0	2	1	1	2	2	0	2	0	2	0	2	2	2	1	0	0	0	0	0	21	
OFFSPRING 3	S1	C13	C6A	C18A	C9	C6B	C18B	C11	C2	C7	C8	C15	C20	C5	C4	C14	C16	C17	C19	C10	C3	C1	C12	TOTAL		
F.F.	1	1	0	0	2	0	0	1	1	2	0	0	0	2	0	0	2	2	0	1	0	0	0	15		

steps, paying attention to the precedence relationships between the components, adjusting the sequences to make them realistically feasible. Figure Figure 12 shows the values for the lowest fitness function

Finally, Figure Figure 13 shows the optimal sequence generated by the GA based on blocks.

2.1.3. Alternative Sequence

An additional disassembly sequence was gathered; by thinking if physically the real mechanical assembly had to disassemble and thought about what it would be necessary to minimize the time. Some technical aspects were taken such as minimizing the number of times the tool is changed, the number of movements of the operator, the number of movements of the assembly and the convenience in removing a component, therefore the space available for maneuver it

1) First, to remove the fixing screws between the upper and lower casing. Proceeding along the perimeter of the casing without paying attention to the diameter of the screws; otherwise, to minimize tool changes, all screws would be handled with the same diameter at a time. For simplicity its assumed to not having an adjustable wrench.

2) After removing the screws, the upper casing is removed to have all the components of the gearbox in view.

3) Remove the six covers in order, along the perimeter of the reducer.

Figure 11. Sequence to find the lowest fitness function.

SEQUENCE 1	S1	C13	C5	C14	C16	C4	C17	C1	C6A	C18A	C9	C6B	C18B	C11	C2	C7	C15	C20	C8	C19	C10	C3	C12	TOTAL
F.F.	1	1	2	0	0	2	1	1	0	0	2	0	0	1	1	2	0	0	2	0	1	0	0	17
OFFSPRING 3	S1	C13	C6A	C18A	C9	C6B	C18B	C11	C2	C7	C15	C20	C8	C5	C14	C16	C4	C17	C19	C10	C3	C1	C12	TOTAL
F.F.	1	1	0	0	2	0	0	1	1	2	0	0	0	2	0	0	2	2	0	1	0	0	0	15

MUTATION OPERATIONS FOR THE "SEQUENCE 1" CHROMOSOME:
 Selection of "chromosome point" C17

SEQUENCE 1	S1	C13	C5	C14	C16	C4	C1	C6A	C18A	C9	C6B	C18B	C11	C2	C7	C15	C20	C8	C19	C10	C3	C12	TOTAL	
F.F.	1	1	2	0	0		1	0	0	2	0	0	0	1	1	2	0	0	2	0	1	0	0	17

Range for insertion: between C4 and C1 -> Cannot be moved
 Selection of "chromosome point" C7

SEQUENCE 1	S1	C13	C5	C14	C16	C4	C17	C1	C6A	C18A	C9	C6B	C18B	C11	C2	C15	C20	C8	C19	C10	C3	C12	TOTAL
F.F.	1	1	2	0	0	2	1	1	0	0	2	0	0	1		0	0	2	0	1	0	0	17

Range for insertion: between C13 and C15
 Noticed: fitness function would not improve wherever is put
 Mutation operations for chromosome "SEQUENCE 1" concluded

MUTATION OPERATIONS FOR THE "OFFSPRING 3" CHROMOSOME:
 Selection of "chromosome point" C17

OFFSPRING 3	S1	C13	C6A	C18A	C9	C6B	C18B	C11	C2	C7	C8	C15	C20	C5	C4	C14	C16	C19	C10	C3	C1	C12	TOTAL
F.F.	1	1	0	0	2	0	0	1	1	2	0	0	0	2	0	0	0	2	1	0	0	0	13

Range for insert: between C5 and C1

OFFSPRING 3	S1	C13	C6A	C18A	C9	C6B	C18B	C11	C2	C7	C8	C15	C20	C5	C4	C14	C16	C19	C10	C17	C3	C1	C12	TOTAL
F.F.	1	1	0	0	2	0	0	1	1	2	0	0	0	2	0	0	0	0	2	1	0	0	0	13

Selection of "chromosome point" C7

OFFSPRING 3	S1	C13	C6A	C18A	C9	C6B	C18B	C11	C2	C8	C15	C20	C5	C4	C14	C16	C19	C10	C17	C3	C1	C12	TOTAL
F.F.	1	1	0	0	2	0	0	1		0	0	0	2	0	0	0	0	2	1	0	0	0	13

Range for insert: between C13 and C15

OFFSPRING 3	S1	C13	C6A	C18A	C7	C9	C6B	C18B	C11	C2	C8	C15	C20	C5	C4	C14	C16	C19	C10	C17	C3	C1	C12	TOTAL
F.F.	1	1	0	0	0	2	0	0	1	1	0	0	0	2	0	0	0	0	2	1	0	0	0	11

Mutation operations for chromosome "OFFSPRING 3" concluded

Figure 12. Top view of disassembly.

SEQUENCE with lower fitness function:

SEQUENCE	S1	C13	C6A	C18A	C7	C9	C6B	C18B	C11	C2	C8	C15	C20	C5	C4	C14	C16	C19	C10	C17	C3	C1	C12	TOTAL
F.F.	1	1	0	0	0	2	0	0	1	1	0	0	0	2	0	0	0	0	2	1	0	0	0	11

Figure 13. Optimal sequence.

DISASSEMBLY EVALUATION CHART																							
TASK No.	PART No.	TASK	TOOL	DISASSEMBLY FORCE					MATERIAL HANDLING			REQUIREMENT OF TOOLS		ACCESSIBILITY OF JOINTS		POSITIONING	TOTAL TASK	NOTE					
				Push/pull operations with hand	Twisting and push/pull op. with hand	Inter surface friction	Inter-surface wedging	material stiffness	Component size	Component weight	Component symmetry	Force exertion	Torque exertion	Dimensions	Locations				Accuracy tool placement				

4) By holding an oil seal extractor tool, both shafts from the sealing rings are taken out for the lubricating oil, so as not to have to use this tool again at a later time.

5) Following the philosophy of minimizing tool change, all six bearings were taken out from the shafts in the assembly.

6) As a last step, the three spacers and the shafts were removed. So only the lower casing and my disassembly operation ends were left.

Finally, the sequence obtained is:

Figure 14. Disassembly evaluation chart.

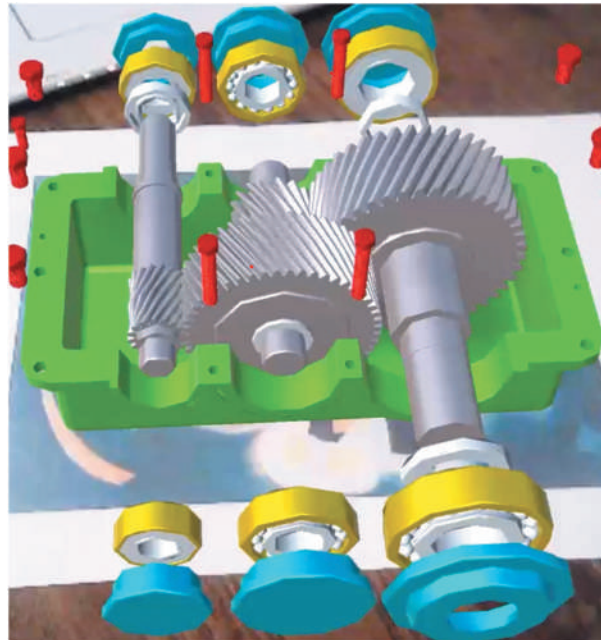
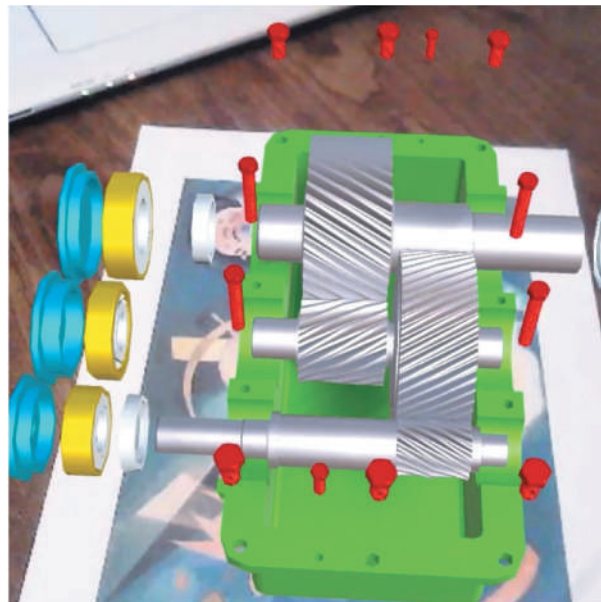


Figure 15. Leftmost side view of disassembly sequence AR simulation sequence AR simulation.



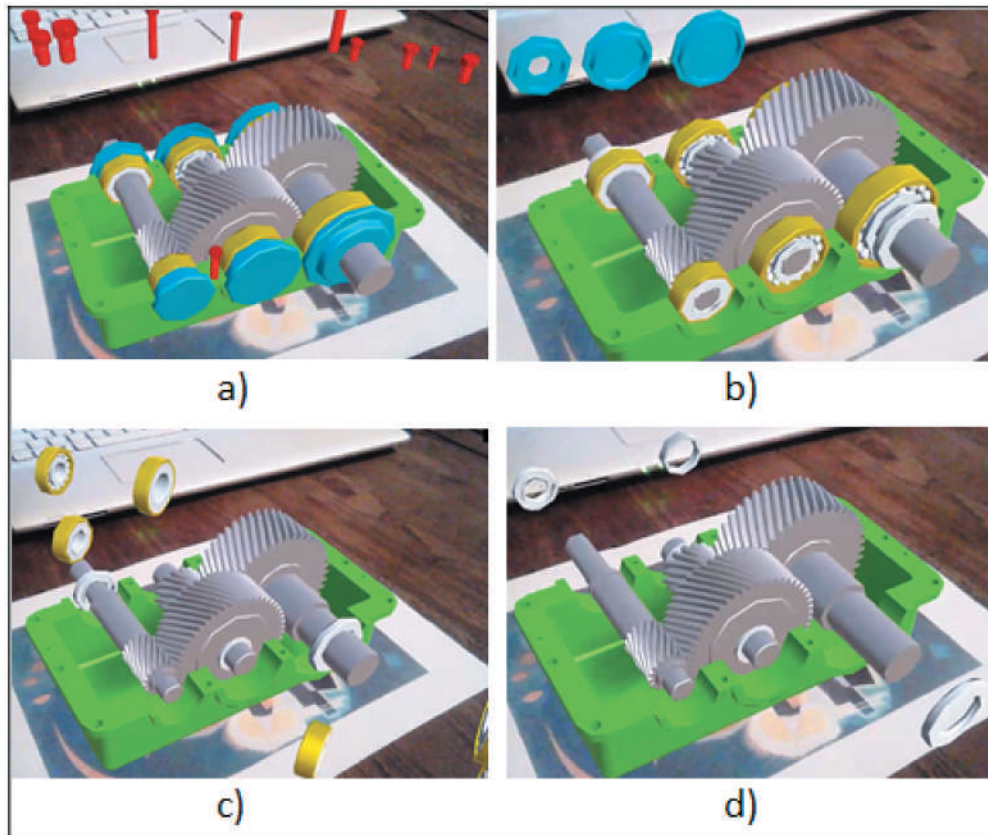
S1-C13-C4-S5-C8-C15-C14-C16-C18a-S19-C18b-C17-C11-C10-C9-C1-C2 -C3.

Sequence obtained that includes subsequences S1, that contains: C21, C22, C23; S5 that contains C5, C6a, C6b, C7; and S19 including C19, C20.

2.1.4. Time and Evaluation Calculation

As previously mentioned, for the calculation of the times related to the three sequences found for the speed reducer, considered proposals found in the research of Mandolini et al. (Mandolini et al., 2018), Francia et al. (Francia et al., 2019), Zhang, Lei, et al. (L. Zhang et al., 2021), Zhang et al. (Zhang &

Figure 16. DSP augmented reality detail analysis: a) S1; b) S5; c) C16-C18a-S19-C18b-C17.d) Spacers and axes.



Zhang, 2009), and back to the proposal of Desai et al.(Desai & Mital, 2003). was taken for using a similar time insertion table. Same of which could be seen in Figure Figure 14, and that includes component description, the movement to be performed is evaluated if the disassembly operation sees friction and the material stiffness. In the third part of the table, the simplicity with which a component can be handled is considered, in relation to its size, weight and shape. Then use of tool force or torque is considered. The fifth section, “accessibility of joints”, considers the accessibility of the joints, therefore how easily they are accessible in terms of size and position. Lastly, the third to last and penultimate columns evaluate the accuracy with which the tool must be positioned for disassembly.

It could be seen that an assessment of the shortest total time related to the customized sequence as shown in Table 7, and equal to 2.87 minutes, which differs from the other proposals by tenths or hundredths of a minute.

2.1.5. Augmented reality application

To develop an augmented reality environment, it is necessary to integrate a library called Vuforia which allows the recognition of the visual marker. Unity is a cross-platform graphics engine developed by Unity Technologies, which allows the development of video games and other interactive content, such as architectural visualizations or 3D animations in real time. Vuforia, on the other hand, is an augmented reality Software Development Kit (SDK) for mobile devices that allows the creation of AR applications. It uses computer vision technology to recognize and track planar images and 3D objects in real time.

Table 8. Time evaluation comparison chart for all sequences

Ord.	Model	Results	
1	PSO Method	Total time (TMU)	480.7
		Unit value (TMU)	0.036
		Estimated time (ET) (sec.)	173.052
		ET in minutes	2.8842
	Sequence	C23-C22-C21-C13-C5-C8-C6b-C17-C18b-C15-C11-C20-C4-C7-C19-C10-C14-C6a-C18a-C16-C9-C2-C3-C1	
2	GA Method	Total time (TMU)	485.0
		Unit value (TMU)	0.036
		Estimated time (ET) (sec.)	174.60
		ET in minutes	2.910
	Sequence	S1-C13-C6A-C18A-C7-C9-C6B-C18B-C11-C2-C8-C15-C20-C5-C4-C14-C16-C19-C10-C17-C3-C1-C12	
3	Customized	Total time (TMU)	478.5
		Unit value (TMU)	0.036
		Estimated time (ET) (sec.)	172.26
		ET in minutes	2.871
	Sequence	S1-C13-C4-S5-C8-C15-C14-C16-C18a-S19-C18b-C17-C11-C10-C9-C1-C2 -C3.	

For this, the 3D model was imported into the scene, the entire assembly was exported from Creo Parametric in “.obj” format. Then the file was added to the Unity “Project” window, which can be organized by the user and can be of great help to view all the files useful for the project. To simulate the disassembly of the gearbox, an Animation in the Project window was created and assigned it to the “complete_driver” Game Object, which consists of creating a succession of movements that are recorded and scanned by a timeline where the frame. For each component (or subset of components) a keyframe (frame) in its initial position and another in the final position were defined.

3. Results

Table 8 show the comparison results of time calculation performed by all three sequences envisaged in the study. The sequence with the lowest value was the customized sequence, with ET equal to 2.87 minutes, which differs from the other proposals by tenths or hundredths of a minute.

3.1. Augmented reality application

Moreover, an AR application of the most optimal sequence for disassembly was performed. Results of the disassembly animation performed on the three disassembly sequences analyzed could be seen in Figures 14-16. This approach allowed to technically realize the sequences calculated by each methodology, that, for the matters of this study, was constrained to one operator, so the disassembly sequences were stated as “sequential”, instead of “parallel”. By looking at the AR simulation, it could be noticed how the chosen design showed a flexible approach for assembly and disassembly (ie. Three axes with all individual elements and end covers for each one, that would allow a parallel-like disassembly approach as well). Part interference was verified for each sequence.

4. Discussion

The approach adopted for DSP enabled to realize potential issues related to mechanics element interconnection, also to better understand the structure of the speed reducer. This practical study also was useful to use the Creo Parametric software and connect the assembly made by the later

in an AR visualization tool. Therefore, the huge potential of the use of 3D CAD software has as a tool for design and prototyping, thanks to which the criticalities of a product are immediately evident, allowing to reduce overall time to market.

The study of the disassembly sequences let to be clear about the critical issues related to the design of the disassembly of a component, therefore a customized sequence could be created by means of combining two different theories. This allowed to reach the best sequence for disassembly times, noting significant deviations. the differences of which are negligible due to the low complexity of the speed reducer, which has a Bill of Materials limited to a few types of components. In addition, an additional calculating criterion for the optimal sequence yielded different results, as previously thought by the research team.

Additionally, about augmented reality, allowed to combine software like Unity, that by the Vuforia package for AR. By analyzing this tool, it was able to understand the great potential that augmented reality can have within a company. With this technology, it is possible to attract the attention of customers in a simpler and more direct way because it allows users to experience and learn about the product in a more engaging way. As for disassembly, at this point it is intuitive to imagine a digital manual, with which the user is better able to familiarize himself with the assembly than a traditional paper manual. Seeing the product in augmented reality, it was much easier to perceive the three dimensions, the dimensions of the components, their joints, and the operations to be performed in sequence. It is also possible to think about showing, during the simulation, the tools to use and the simplest way to perform the operations.

Finally, augmented reality could find various applications in different areas within a company. In the element-development projects it allows to intervene in the early stages and eliminate any criticalities. In maintenance, remote assistance and preventive and predictive maintenance activities are improved. In personnel training it is possible to transfer skills to operators in a reality like the actual one. The result is measured in operational efficiency, safety and customer service level.

Acknowledgments

The authors wish to acknowledge the Department of Industrial Engineering of the University of Bologna for the continuous support on research development.

Funding

The authors received no direct funding for this research.

Author details

Leonardo Frizziero¹
ORCID ID: <http://orcid.org/0000-0003-4809-3536>
Giampiero Donnici¹
ORCID ID: <http://orcid.org/0000-0002-6666-1309>
Gian Maria Santi¹
Christian Leon-Cardenas¹
E-mail: christian.leon2@unibo.it
ORCID ID: <http://orcid.org/0000-0002-6430-4615>
Patrich Ferretti¹
Gaia Pascucci¹
Alfredo Liverani¹
ORCID ID: <http://orcid.org/0000-0002-3255-9381>
¹ Department of Industrial Engineering, Alma Mater Studiorum University of Bologna, Viale Risorgimento, 2 – 40136 Bologna, Italy.

Disclosure statement

No potential conflict of interest was reported by the author(s).

Citation information

Cite this article as: Disassembly sequence planning validated thru augmented reality for a speed reducer, Leonardo Frizziero, Giampiero Donnici, Gian Maria Santi,

Christian Leon-Cardenas, Patrich Ferretti, Gaia Pascucci & Alfredo Liverani, *Cogent Engineering* (2022), 9: 2061321.

References

- Anil Kumar, G., Bahubalendruni, M. V. A., Prasad, V. S. S., Sankaranarayanan, K., & Multi-Layered Disassembly, A. (2021). Sequence planning method to support decision making in de-manufacturing. *Sadhana*, 46(2), 1–16. <https://doi.org/10.1007/s12046-021-01622-3>
- Bahubalendruni, M. V. A. R., & Biswal, B. B. (2018). An intelligent approach towards optimal assembly sequence generation. *Proc. Inst. Mech. Eng. Part C J. Mech. Eng. Sci.*, 232(4), 531–541. <https://doi.org/10.1177/0954406216684159>
- Bahubalendruni, M. V. A. R., Gulivindala, A., Kumar, M., Biswal, B. B., Annepu, L. N., & Hybrid Conjugated, A. (2019). Method for assembly sequence generation and explode view generation. *Assem. Autom.*, 39(1), 211–225. <https://doi.org/10.1108/AA-01-2018-014>
- Bahubalendruni, M. V. A. R., Gulivindala, A. K., Varupala, S. S. V. P., & Palavalasa, D. K. (2019). Optimal assembly sequence generation through computational approach. *Sādhana*, 44(8), 1–9. <https://doi.org/10.1007/s12046-019-1157-2>
- Bahubalendruni, M. V. A. R., & Varupala, V. P. (2021). Disassembly sequence planning for safe disposal of end-of-life waste electric and electronic equipment. *Natl. Acad. Sci. Lett.*, 44(3), 243–247. <https://doi.org/10.1007/s40009-020-00994-0>
- Barone, S., Paoli, A., Razionale, A. V., & Berretta, M. (2020). *Disegno Tecnico Industriale*. Città Studi Edizioni.

- Tseng, H.-E., Chang, -C.-C., Lee, S.-C., & Huang, Y.-M. (2018). A Block-Based Genetic Algorithm for disassembly sequence planning. *Expert Systems with Applications*, 96(15 April 2018), 492–505. <https://doi.org/10.1016/j.eswa.2017.11.004>
- Callegari, M., Fanghella, P., & Pellicano, F. (2013). *Meccanica applicata alle macchine*. Città Studi Edizioni.
- Chen, D.-Z., Wei, C., Jia, G.-L., & Hu, Z.-H. (2020). Shortest-path optimization of ship diesel engine disassembly and assembly based on and/or network. *Complexity*, 2020, 15. <https://doi.org/10.1155/2020/2919615>
- Chunming, Z. (2016). Optimization for disassemble sequence planning of electromechanical products during recycling process based on genetic algorithms. *Int. J. Multimed. Ubiquitous Eng*, 11(4), 107–114. <https://doi.org/10.14257/ijmue.2016.11.4.11>
- Desai, A., & Mital, A. (2003). Evaluation of disassemblability to enable design for disassembly in mass production. *Int. J. Ind. Ergon*, 32(4), 265–281. [https://doi.org/10.1016/S0169-8141\(03\)00067-2](https://doi.org/10.1016/S0169-8141(03)00067-2)
- Kheder, M., Trigui, M., & Aifaoui, N. (2018, March 27–29). A Disassembly Sequence Planning Approach Based on Particle Swarm Optimization. Proceedings of the 7th Conference on Design and Modeling of Mechanical Systems, CMSM' 2017, Hammamet, Tunisia (pp. 1017–1025). Springer .
- Dorigo, M., Birattari, M., & Stutzle, T. (2006). Ant colony optimization: artificial ant as a computational intelligence technique. *IEEE Computational Intelligence Magazine*, 1(4), 28–39. <https://doi.org/10.1109/MCI.2006.329691>
- Dowland, K. A., & Thompson, J. (2012). *Handbook of Natural Computing* (Rozenberg, Grzegorz, Back, Thomas and Kok, Joost N), 1623–1655.
- Francia, D., Ponti, S., Frizziero, L., & Liverani, A. (2019). Virtual mechanical product disassembly sequences based on disassembly order graphs and time measurement units. *Appl. Sci*, 9(17), 17. <https://doi.org/10.3390/app9173638>
- Giudice, F., & Fargione, G. (2007). Disassembly planning of mechanical systems for service and recovery: a genetic algorithms based approach. *J. Intell. Manuf*, 18(3), 313–329. <https://doi.org/10.1007/s10845-007-0025-9>
- Gulivindala, A. K., Bahubalendruni, M., Chandrasekar, R., Ahmed, E., Abidi, M. H., & Al-Ahmari, A. (2021). Automated disassembly sequence prediction for industry 4.0 using enhanced genetic algorithm. *Comput. Mater. Contin*, 69(2), 2531–2548. <https://doi.org/10.32604/cmc.2021.018014>
- Gulivindala, A. K., Bahubalendruni, M. V. A. R., Inkulu, A. K., Varupala, S. S. V. P., & SankaranarayanaSamy, K. (2021). A modified cut-set method for mechanical subassembly identification. *Assem. Autom*, 41(6), 659–680. <https://doi.org/10.1108/AA-05-2021-0057>
- Gunji, B. M., Pabba, S. K., Rajaram, I. R. S., Sorakayala, P. S., Dubey, A., Deepak, B., Biswal, B. B., & Bahubalendruni, M. V. A. R. (2021). Optimal disassembly sequence generation and disposal of parts using stability graph cut-set method for end of life product. *Sādhanā*, 46(1), 1–15. <https://doi.org/10.1007/s12046-020-01525-9>
- Guo, J., Zhong, J., Li, Y., Du, B., & Guo, S. (2019). A hybrid artificial fish swam algorithm for disassembly sequence planning considering setup time. *Assem. Autom*, 39(1), 140–153. <https://doi.org/10.1108/AA-12-2017-180>
- Hao, W., & Hongfu, Z. (2009). Using genetic annealing simulated annealing algorithm to solve disassembly sequence planning. *J. Syst. Eng. Electron*, 20(4), 906–912. <https://ieeexplore.ieee.org/abstract/document/6074518>
- Herotech srl. La Realtà Aumentata nelle aziende. <https://www.arealitymarket.com/la-realta-aumentata-nelle-aziende/> (accessed Dec 6, 2020).
- Holland, J. H. (1992). *Adaptation in natural and artificial systems: an introductory analysis with applications to biology, control, and artificial intelligence*. MIT press.
- Hu, Y., & Ameta, G. (2019). Approach to estimate disassembly time: hypothesis, model and validation. *J. Manuf. Sci. Eng*, 141(2), Article 021009. <https://doi.org/10.1115/1.4042107>
- Hu, Q., Qiao, L., & Peng, G. (2017). An ant colony approach to operation sequencing optimization in process planning. *Proceedings of the Institutions of Mechanical Engineers: Part B Journal of Engineering Manufacturing*, 231(3), 470–489. <https://doi.org/10.1177/0954405415616786>
- Kheder, M., Trigui, M., & Aifaoui, N. (2017). Optimization of disassembly sequence planning for preventive maintenance. *The International Journal, Advanced Manufacturing Technology*, 90(5), 1337–1349. <https://doi.org/10.1007/s00170-016-9434-2>
- Kim, H.-W., Park, C., & Lee, D.-H. (2018). Selective disassembly sequencing with random operation times in parallel disassembly environment. *International Journal of Production Research*, 56(24), 7243–7257. <https://doi.org/10.1080/00207543.2018.1432911>
- Lambert, A. J. D. (2003). Disassembly Sequencing: A Survey. *International Journal of Production Research*, 41(16), 3721–3759. <https://doi.org/10.1080/0020754031000120078>
- Luo, Y., Peng, Q., & Gu, P. (2016). Integrated multi-layerrepresentation and ant colony search for product selective disassembly planning. *Computers in Industry*, 75(January 2016), 13–26. <https://doi.org/10.1016/j.compind.2015.10.011>
- Mandolini, M., Favi, C., Germani, M., & Marconi, M. (2018). Time-Based disassembly method: how to assess the best disassembly sequence and time of target components in complex products. *The International Journal, Advanced Manufacturing Technology*, 95(1), 409–430. <https://doi.org/10.1007/s00170-017-1201-5>
- Marconi, M., Germani, M., Mandolini, M., & Favi, C. (2019). Applying data mining technique to disassembly sequence planning: a method to assess effective disassembly time of industrial products. *International Journal of Production Research*, 57(2), 599–623. <https://doi.org/10.1080/00207543.2018.1472404>
- Meng, W., & Zhang, X. (2020). Optimization of remanufacturing disassembly line balance considering multiple failures and material hazards. *Sustainability*, 12(18), 7318. <https://doi.org/10.3390/su12187318>
- Mitrouchev, P., Wang, C. G., Lu, L. X., & Li, G. Q. (2015). Selective disassembly sequence generation based on lowest level disassembly graph method. *The International Journal, Advanced Manufacturing Technology*, 80(1), 141–159. <https://doi.org/10.1007/s00170-015-6861-4>
- Kumar, G. A., Bahubalendruni, M. V. A. R., Prasad, V. S. S. V., Ashok, D., & Sankaranarayanasamy, K. (2021). A Novel Geometric feasibility method to perform assembly sequence planning through oblique orientations. *Engineering Science and Technology, an International Journal*, 26 (February 2022), Article 100994. <https://doi.org/10.1016/j.jestch.2021.04.013>
- Poli, R., Kennedy, J., & Blackwell, T. (2007). Particle Swarm Optimization. *Swarm Intell*, 1(1), 33–57. <https://doi.org/10.1007/s11721-007-0002-0>
- Poole, D. L., & Mackworth, A. K. (2010). *Artificial intelligence: foundations of computational agents*. Cambridge University Press.

- Pornsing, C., & Watanasungsuit, A. (2014, September 23–25). *Discrete particle swarm optimization for disassembly sequence planning*. IEEE International Conference on Management of Innovation and Technology; IEEE, Singapore, (pp. 480–485). <https://doi.org/10.1109/ICMIT33147.2014>
- Rickli, J. L., & Camelio, J. A. (2013). Multi-Objective Partial Disassembly Optimization Based on Sequence Feasibility. *J. Manuf. Syst*, 32(1), 281–293. <https://doi.org/10.1016/j.jmsy.2012.11.005>
- Rickli, J. L., & Camelio, J. A. (2014). Partial disassembly sequencing considering acquired end-of-life product age distributions. *International Journal of Production Research*, 52(24), 7496–7512. <https://doi.org/10.1080/00207543.2014.939237>
- RS Components S.r.l. *Guida completa sui Motoriduttori* <https://it.rs-online.com/web/generalDisplay.html?id=idee-suggerimenti/guida-motoriduttore> (accessed Dec 20, 2020)
- Shuyi, Y., Jingjing, L., Zejun, W., Zhongju, H., & Wenhui, Y. (2014). Research on disassembly sequence planning for transfer case of concrete pump. *Machine Design and Research*, 2014(5), 106–109+124. http://caod.oriprobe.com/articles/45773407/Research_on_Disassembly_Sequence_Planning_for_Transfer_Case_of_Concret.htm
- Smith, S., Hsu, L.-Y., & Smith, G. C. (2016). Partial disassembly sequence planning based on cost-benefit analysis. *Journal of Cleaner Production*, 139(15 December 2016), 729–739. <https://doi.org/10.1016/j.jclepro.2016.08.095>
- Van Zanten, A. J. (1997). Lexicographic Order and Linearity. *Des. Codes Cryptogr*, 10(1), 85–97. <https://doi.org/10.1023/A:1008244404559>
- Wang, J., Wu, X., Fan, X., & Two-Stage Ant, A. (2015). Colony optimization approach based on a directed graph for process planning. *The International Journal, Advanced Manufacturing Technology*, 80(5), 839–850. <https://doi.org/10.1007/s00170-015-7065-7>
- Xu, J., Zhang, S.-Y., & Fei, S.-M. (2011). Product remanufacture disassembly planning based on adaptive particle swarm optimization algorithm. *J. Zhejiang Univ. (Engineering Sci)*, 45(10), 1746–1752. <https://www.zjujournals.com/eng/Y2011/V45/110/1746>
- Zhang, N., Liu, Z., Qiu, C., Cheng, J., & Tan, J. (2020). Disassembly sequence planning using a fast and effective precedence-based disassembly subset-generation method. *Proceedings of the Institutions of Mechanical Engineers: Part B Journal of Engineering Manufacturing*, 234(3), 513–526. <https://doi.org/10.1177/0954405419870966>
- Zhang, Y., Wang, S., & Ji, G. (2009). A Comprehensive Survey on Particle Swarm Optimization Algorithm and Its Applications. *Mathematical Problems in Engineering*, 2015(1), Article 931256. <https://doi.org/10.1155/2015/931256>
- Zhang, X., Wang, S., Yi, L., Xue, H., Yang, S., & Xiong, X. (2018). An integrated ant colony optimization algorithm to solve job allocating and tool scheduling problem. *Proceedings of the Institutions of Mechanical Engineers: Part B Journal of Engineering Manufacturing*, 232(1), 172–182. <https://doi.org/10.1177/0954405416636038>
- Zhang, L., Wu, Y., Li, Z., Zheng, Y., Ren, Y., & Zhu, L. (2021). A systematic approach in remanufacturing for high efficiency and low cost: the selective parallel disassembly sequence planning. *Proceedings of the Institutions of Mechanical Engineers: Part B Journal of Engineering Manufacturing*, 236(5), 572–585. <https://doi.org/10.1177/09544054211041036>
- Zhong, L., Youchao, S., Gabriel, O. E., & Haiqiao, W. (2011). Disassembly sequence planning for maintenance based on metaheuristic method. *Aircr. Eng. Aerosp. Technol*, 83(3), 138–145. <https://doi.org/10.1108/00022661111131221>



© 2022 The Author(s). This open access article is distributed under a Creative Commons Attribution (CC-BY) 4.0 license.

You are free to:

Share — copy and redistribute the material in any medium or format.

Adapt — remix, transform, and build upon the material for any purpose, even commercially.

The licensor cannot revoke these freedoms as long as you follow the license terms.

Under the following terms:

Attribution — You must give appropriate credit, provide a link to the license, and indicate if changes were made.

You may do so in any reasonable manner, but not in any way that suggests the licensor endorses you or your use.

No additional restrictions

You may not apply legal terms or technological measures that legally restrict others from doing anything the license permits.

***Cogent Engineering* (ISSN: 2331-1916) is published by Cogent OA, part of Taylor & Francis Group.**

Publishing with Cogent OA ensures:

- Immediate, universal access to your article on publication
- High visibility and discoverability via the Cogent OA website as well as Taylor & Francis Online
- Download and citation statistics for your article
- Rapid online publication
- Input from, and dialog with, expert editors and editorial boards
- Retention of full copyright of your article
- Guaranteed legacy preservation of your article
- Discounts and waivers for authors in developing regions

Submit your manuscript to a Cogent OA journal at www.CogentOA.com

